The International Archives of the Photogrammetry, Remote Sensing and Spatial Information Sciences, Volume XLVIII-M-9-2025
30th CIPA Symposium “Heritage Conservation from Bits:
From Digital Documentation to Data-driven Heritage Conservation”, 25–29 August 2025, Seoul, Republic of Korea

Digital Damage Measurement and Analysis of Masonry Heritage Based on Degradation Measurement Method (MMD)

Jun Cai[1], Jianfei Dong[1], Hao Wang[2], Sheng Huang[1]

[1] School of Architecture and Design, Harbin Institute of Technology, China； Key Laboratory of Cold Region Urban and Rural Human Settlement Environment Science and Technology Ministry of Industry and Information Technology – China.326445856@qq.com, dongjianfei999@hotmail.com, 821498578@qq.com
[2] Palace Museum of the Manchurian Regime, China – 88406699@qq.com

Keywords: Masonry Heritage, Degradation Measurement Method (MMD), Damage Atlas, Damage Factor, Digital Conservation Technology.

Abstract

Preventive conservation of architectural heritage is a crucial component of heritage preservation efforts.The measurement and analysis of damage data in architectural heritage facilitate early assessment of damage severity and the development of appropriate preventive and restoration strategies.This study focuses on modern masonry architectural heritage, using Jixi Building of the Puppet Manchurian Palace Museum in Changchun, China as a case study. Three-dimensional laser scanning technology is employed to collect damage data of facade materials, which are then translated and visualized through the generation of a damage atlas.We apply the Degradation Measurement Method (MMD) to conduct statistical and quantitative analysis of facade material damage in architectural heritage. Its innovation lies in the real-time acquisition and analysis of damage data to reveal the spatial distribution patterns of defects, and in the calculation of damage factors to objectively assess the health condition of masonry facade materials. As a digital damage measurement and analysis technique, the application of MMD in the field of architectural heritage conservation enables timely investigation of facade damage, saving valuable response time and significantly reducing the consumption of human and material resources, while providing data-based support for restoration design; through the use of timely dynamic data to evaluate the effectiveness of restoration strategies, it improves the predictive efficiency of restoration implementation and holds significant scientific value for the preventive conservation of heritage damage and the management of historic buildings.

1. Introduction

Architectural heritage stands as a testament to the development of human civilization, bearing the memory of history and the continuity of culture. Among various forms of architectural heritage, masonry heritage has consistently been a focal point of cultural conservation due to its unique artistic value and historical significance. Over years of alternating hot and cold climates, exposure to wind and sunlight, and changes in function, both the surface materials and internal structures of architectural heritage have sustained varying degrees of damage. Accurately diagnosing the preservation condition of architectural heritage forms the basis of all restoration and conservation efforts. Conducting objective pathological diagnosis and health assessment of heritage buildings is essential for formulating targeted repair strategies and has become a major research focus in recent years. As the primary protective barrier of architectural heritage, facade materials are subjected to long-term exposure to adverse environmental conditions and respond with distinct pathological manifestations depending on the type of erosion, which has a significant impact on the overall health of the heritage structure. Conducting regular inspections of the facade system and identifying anomalies are fundamental to decision-making in restoration interventions.

Accurate acquisition of damage data in architectural heritage is a critical foundation for effective damage diagnosis, and Terrestrial Laser Scanning (TLS) is currently one of the most precise methods for such data collection, offering advantages such as speed, accuracy, high point cloud density, non-contact measurement, and insensitivity to lighting conditions, and has been widely applied in the conservation of historic buildings. Many scholars and research institutions have conducted in-depth studies on TLS and successfully applied it in the protection of historic buildings. For example, Michael et al. used a terrestrial laser scanner to collect data on the Bamiyan Buddhas in Afghanistan and constructed 3D models for the purpose of virtual restoration(Jansen et al., 2008). The Palace Museum in Beijing, China, used TLS to carry out digital research and archiving of the Nansansuo historic building complex within the Forbidden City(Wang, 2011).

Infrared thermography is a non-destructive testing tool based on the principle of thermal radiation, with the advantage of detecting hidden defects in architectural heritage—such as cracks, voids, moisture, or material degradation—by identifying temperature differences. By integrating infrared thermography with TLS, a comprehensive diagnosis ranging from macroscopic form to microscopic defects can be achieved, offering a scientific basis for decision-making in cultural heritage conservation. For example, Ecem Edis et al. conducted field investigations and numerical simulations on moisture issues in tiled facades, applying infrared thermography to detect moisture in facing bricks and achieving promising results(Edis et al., 2014). Panagiotis Theodorakeas et al. evaluated the role of active cooling thermography in revealing and quantitatively describing defects in mosaic layers through experiments and numerical simulations(Theodorakeas et al., 2014).

This study applies digital measurement technologies and analytical methods to collect damage information of facade

materials and quantitatively assess the health condition of architectural heritage through non-destructive and low-cost means, providing a scientific basis for the management and restoration of heritage buildings, and addressing a critical gap in current heritage conservation practices.

2. Methods

2.1 Damage Atlas

The damage atlas serves as a foundational document in the restoration and conservation of architectural heritage, integrating information on the damage condition of heritage structures and is considered a qualitative analysis method(Silveira da Costa et al., 2021). Creating a damage atlas is a preliminary task in architectural heritage restoration projects. Pedro Gaspar from the Faculty of Architecture at the Technical University of Lisbon proposed a probability and sensitivity analysis map for facade mortar coating degradation in 2005 (Figure 1-a)(Gaspar & de Brito, 2005). Maja Frankovic from the Central Institute for Conservation in Belgrade, Serbia, created a color-coded graphical representation (Figure 1-b) to identify the intensity of damage observed in cultural heritage sites (Franković et al., 2015). Sarah Janvier-Badosa from the UMR Materials Research Center in France chose to draw damage maps directly on facade images (Figure 1-c), using a robotic platform equipped with a digital camera to capture the images, which were then orthorectified through photogrammetry(Janvier- Badosa et al., 2013).

(a) (b) (c)

Figure 1. Graphical Representations of Damage Mapping Methods

An analysis of current international literature reveals that no unified standard has yet been established across countries for the mapping of damage and deterioration in architectural heritage. From the existing literature, several characteristics can be summarized regarding how scholars internationally represent damage in their outputs: a. Damage atlases that display the complete facade view are more intuitive than those showing only partial sections, as they allow for a clearer perception of the degradation state of facade materials. b. Orthophotos assist in identifying the locations of damage, but the image processing workflow may result in the loss or distortion of material damage information. c. Using different colors in accurate graphic files to represent types and severity of damage is a highly effective mapping approach, as it clearly illustrates the progression of degradation and supports conservation and maintenance efforts.

In addition, the graphical representation provided by the damage atlas must be clear and comprehensible to ensure that all relevant professionals can interpret it accurately. At the same time, the damage map should allow for measurement recording; to maximize the visual clarity of the represented defects, it is recommended that textual elements be minimized within the atlas(Carvalho, 2018). In summary, the approach to damage atlas construction in this study draws upon representation methods found in the latest internationally published research on architectural heritage damage mapping.

2.2 Degradation Measurement Method (MMD)

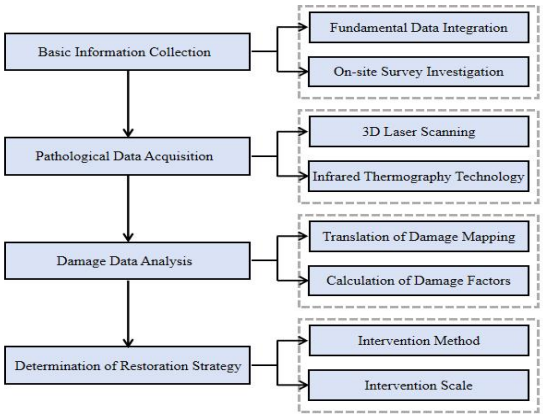

Figure 2. Schematic Diagram of the MMD Process

In 2014, Dr. Silva from the University of Brasília proposed a method for measuring material damage in buildings—known as the Degradation Measurement Method (MMD)—and developed a model to calculate facade damage levels, thereby providing a data foundation for subsequent interventions in architectural heritage(Silva, 2014). MMD is a method developed through the study of various cases of building degradation, establishing correlations between quantitative values referred to as degradation indices to characterize facade damage. Over the past decade, numerous international scholars have built upon Dr. Silva’s work by conducting supplementary research on the MMD method, which has been widely applied to various architectural heritage cases across different countries. In 2016, De Souza et al. used the MMD method to determine the intensity and distribution of damage across different facade regions(De Souza et al., 2016). The results indicated that for comparative analysis between regions, the observed values should be adjusted according to the proportion of each region's area relative to the total facade area. In 2020, Bauer et al. further refined the MMD method and proposed guidelines for anomaly inspection, mapping, quantification procedures, and indicator calculation(Bauer et al., 2020a). Bauer, De Souza, and Piazzarollo used the MMD method to analyze pathologies in facade plastering by mapping the observed pathological damage during field surveys and correlating these conditions with their probable causes and impacts on system performance(Bauer et al., 2020b). It is evident that over more than a decade of international development, the MMD has been progressively refined and has matured into an effective foundational research method for quantifying damage levels in architectural heritage. Therefore, the main objective of this study is to propose a method for quantifying specific types of damage in masonry heritage based on the principal damage patterns identified during surveys, which is essential for determining the scale of intervention and selecting appropriate restoration strategies (Figure 2).

2.3 Damage Index Calculation

The MMD method evaluates the overall damage level of architectural heritage by calculating the damage coverage rate, which refers to the ratio between the area affected by various pathological manifestations and the total facade area. The calculation of the total damage coverage rate—i.e., the sum of all types of damage coverage—is a key factor in damage assessment. Based on the adjustment of the existing damage atlas and the application of a grid overlay, the process involves several steps: quantification of damage areas, calculation of the Damage Factor (FD) and Total Damage Factor (FDt), subdivision of the facade into regions, computation of Regional

Damage Factors (FDr), determination of the Regional Correction Coefficient (CCr), and calculation of the Corrected Regional Damage Factor (FDrc).

It is important to emphasize that, in this study, the measurement of material-related damage excludes the damage conditions of infill components around facade openings—such as glass windows, shutters, and doors—which are considered replaceable elements. Therefore, in the application of the MMD method, the facade area used for damage factor calculations refers to the net facade area, defined as the total facade area minus the area of openings. This is hereinafter referred to as the facade area.

2.3.1 Adjustment of the Damage Atlas: First, adjustments were made to the damage atlas to remove secondary damage types—such as vegetation coverage and minor surface soiling—that have minimal impact on the health condition of the heritage structure.Based on Dr. Silva’s doctoral dissertation, several grid sizes were analyzed, including 1.60 m × 1.60 m, 1.00 m × 1.00 m, 0.70 m × 0.70 m, and 0.50 m × 0.50 m.Through adjustments during the mapping process, it was found that the buildings in Dr. Silva’s case studies were larger in scale than those in the present study, making the original grid sizes too large.Therefore, to better evaluate pathological manifestations, this study adopted customized smaller grids and tested grid sizes of 0.50 m × 0.50 m, 0.30 m × 0.30 m, 0.10 m × 0.10 m, and 0.05 m × 0.05 m.Basesd on the grid analysis, the 0.05 m × 0.05 m grid provided approximations that were closer to the actual damage conditions and enabled better quantification of anomalies.

2.3.2 Delineation of Damage Areas: The MMD method divides the facade of architectural heritage into six damage zones: Cantilevered Elements (such as balconies and verandas), areas surrounding Openings (doors, windows, etc.), Corners and Edges, Interstory Transition Zones, Parapet Walls, and Continuous Walls.Each delineated facade zone presents varying area sizes due to differences in typological characteristics.Because the quantifiable area of each target zone differs, it is necessary to establish a weighting factor—referred to as the CCr—to calibrate the damage level across zones, taking into account the specific extent of damaged area in each region.Each representative zone (including Continuous Walls, Openings, Cantilevered Elements, Corners and Edges, joints, and tops) is separated by Interstory Transition Zones—the smallest in area—and proportionally greater weight should be assigned to the smaller regions.

2.3.3 Quantification of Injury Symptoms and Size: The quantification of damage area is carried out under the condition that damage is present within the grid (affected area).The FD is defined as the ratio of the total damaged area corresponding to each anomaly to the total facade area.The formula is as follows:

$$FD = \frac{A_{\mathrm{d}(n)}}{A_t} \quad (1)$$

where FD = the facade Damage Factor
$A_{\mathrm{d}(n)}$ = the damaged area of a specific type on the facade
A_t= the total sample area of the facade

The FDt is defined as the sum of all individual damage factors on the same facade.The formula is as follows:

$$FDt = \Sigma FD \quad (2)$$

where FDt = the Total Damage Factor of the facade

After calculating FD and FDt, the measured building facade is subdivided into zones—namely Cantilevered Elements (e.g., balconies), Openings, Corners and Edges, Interstory Transition Zones, Parapet Walls, and Continuous Walls—as shown in Figure 3; then, the FDr is calculated. The formula is as follows:

$$FDr = \sum \frac{Ar}{At} \quad (3)$$

where Ar= the total area of all damage types within a specific region
A_t= the total sample area of the facade

FDr accounts for the anomalous regions within each facade and includes all damage present in the corresponding grid cells.Its results may exhibit distortion when directly influenced by the size of the analyzed region, and therefore require adjustment and normalization.Within the same facade, some zones may cover significantly larger areas than others, which can distort the analysis of damage incidence—larger zones may appear to have a higher degradation rate compared to smaller ones.Therefore, the CCr is applied to adjust for this discrepancy; it is defined as the ratio between the area of the smallest region and that of the region under analysis.The formula is as follows:

$$CCr = \frac{Ar(m)}{Ar(x)} \quad (4)$$

where CCr= the Regional Correction Coefficient
$Ar(m)$= the area of the smallest region
Ar(x)= the area of the region under analysis

Finally, the FDrc is used to calculate the degradation level of specific regions and to obtain the most accurate approximation of actual damage recurrence within those regions.The formula is as follows:

$$FDrc = \left(\frac{\Sigma Ar(n)}{A_t}\right) \times CCr \quad (5)$$

where FDrc= the Corrected Regional Damage Factor
$\Sigma Ar(n)$ = the total damaged area within a specific region
At= the total sample area of the facade
CCr = the Correction Coefficient of the analyzed region

3. Case Analysis

This study selects the Jixi Building within the Puppet Manchurian Palace Museum in Changchun, China, as the practical case.Originally constructed in 1908 and reconstructed in 1928, the building comprises two above-ground stories and one basement level. It is currently designated as a national-level cultural heritage site in China. The structural system is brick-wood, and the envelope material consists of exposed blue brick masonry.The facade is symmetrically arranged, with both wings projecting approximately 1.25 meters from the central mass.The central entrance of the south facade is designed with a gable facing south, above which a circular brick-arched window is set at the apex of the triangular gable, serving both decorative and ventilation purposes.The building has undergone six different degrees of renovation since 1964, the most recent of which was in 2017. However, in recent years, the facade materials of buildings have been gradually exposed to varying degrees of material damage, driven by harsh climatic environments and improper maintenance.

The colored point cloud model obtained through terrestrial laser scanning can constrain measurement errors to the millimeter scale, while unmanned aerial vehicles (UAVs) equipped with laser scanners can capture data from concealed locations, allowing the measured building dimensions and

damage dimensions to closely approximate reality.In this study, a VLX wearable laser scanner was used in combination with oblique photogrammetry captured by a DJI Mavic 3T UAV to collect facade data of the Jixi Building.

(a) South Facade Point Cloud (b) East Facade Point Cloud

(c) North Facade Point Cloud (d) West Facade Point Cloud

Figure 3. Facade Point Clouds of the Jixi Building

The point cloud model provides accurate dimensional data of damage in architectural heritage; however, the corresponding software tools typically allow only data reading, without direct support for computation or statistical analysis.Therefore, AutoCAD software is used to import the processed point cloud data and transfer the corresponding damage information onto architectural facade drawings, thereby enabling the visualization of damage data.

After processing the infrared thermographic data of the Jixi Building, an infrared thermal image of the building’s exterior facade was obtained (Figure 4). As the overall envelope structure of the building follows a consistent design, the surface temperature across areas composed of the same material should theoretically be uniform in the thermal image; therefore, significant temperature anomalies can qualitatively indicate structural differences within the envelope system.

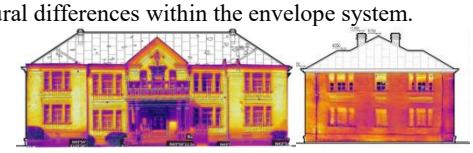

(a) South Facade (b) West Facade

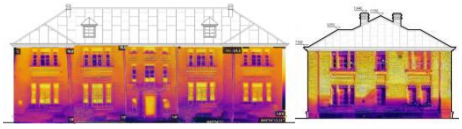

(c) North Facade (d) East Facade

Figure 4. Infrared Thermal Images of the Facades of the Jixi Building

4. Results and Discussion

4.1 Statistical Analysis of Damage Extent

The damage atlases for the south, north, east, and west facades of the Jixi Building were generated, as shown in Figures 5–8, with the corresponding damage extents presented in Tables 1–4.

Based on the damage data from each facade, it can be observed that variations in physical conditions and patterns of human use have led to different dominant pathological manifestations across facades, and notably, significant differences also exist between the upper and lower portions of the same facade.The occurrence rate of cracks in the Interstory Transition Zones across facades is relatively low, suggesting that changes in the internal structure are not the main cause of material-related cracks in the external wall.As the prevailing wind direction in Changchun is northwesterly throughout the year, the north facade experiences the most severe deterioration, with more pronounced powdering and efflorescence.Overall, soiling is primarily concentrated on the wall sections below windows.Apart from improper human use, this phenomenon can be interpreted — according to Professor Sousa of the Technical University of Lisbon — as being related to moisture sources(Sousa et al., 2011).Since the wall beneath the window is close to the ground, moisture is drawn upward by capillary action and carries with it a large amount of ground dust.As moisture evaporates under sunlight while the dust remains, long-term accumulation leads to the buildup of surface soiling.Of course, the occurrence of soiling on the shaded sides of the building involves more than just this process.Capillary action facilitates moisture transport, and the limited exposure to direct sunlight creates favorable conditions for the growth of mold and bacteria, resulting in the accumulation of stains.

South Facade	Facade Area (m^2)		187.307	
Pathological Type	Indicated Area in Damage Atlas(m^2)	Number of Instances	Damage Coverage Rate (%)	Total Damage Coverage Rate (%)
Crack	0.025	15	0.013	9.158 (excluding Fading)
Weathering	12.861	45	6.866	
Powdering	0.147	26	0.078	
Spalling	0.28	19	0.149	
Soiling	0.4	7	0.214	
Fading	0.535	2	0.286	
Material Loss	0.07	5	0.037	
Efflorescence	3.37	165	1.799	

Table 1. Overview of Damage Extent on the South Facade

North Facade	Facade Area (m^2)		177.329	
Pathological Type	Indicated Area in Damage Atlas(m^2)	Number of Instances	Damage Coverage Rate (%)	Total Damage Coverage Rate (%)
Crack	0.015	18	0.008	7.478 (excluding Fading)
Weathering	9.636	69	5.434	
Powdering	0.89	124	0.502	
Spalling	0.723	29	0.408	
Soiling	1.251	7	0.705	
Fading	1.669	4	0.941	
Material Loss	0.066	10	0.037	
Efflorescence	0.68	301	0.383	

Table 2. Overview of Damage Extent on the North Facade

East Facade	Facade Area (m^2)		111.719	
Pathological Type	Indicated Area in Damage Atlas(m^2)	Number of Instances	Damage Coverage Rate (%)	Total Damage Coverage Rate (%)
Crack	0.01	14	0.009	7.576 (excluding Fading)
Weathering	7.045	32	6.306	
Powdering	0.452	46	0.405	
Spalling	0.074	5	0.066	
Soiling	0.329	1	0.294	
Fading	0	0	0.000	
Material Loss	0.02	11	0.018	
Efflorescence	0.534	136	0.478	

Table 3. Overview of Damage Extent on the East Facade

West Facade	Facade Area (m^2)		111.92	
Pathological Type	Indicated Area in Damage Atlas(m^2)	Number of Instances	Damage Coverage Rate (%)	Total Damage Coverage Rate (%)
Crack	0.007	8	0.006	9.196 (excludin
Weathering	4.792	15	4.282	

Powdering	0.399	39	0.357	g Fading)
Spalling	0.151	38	0.135	
Soiling	3.609	8	3.225	
Fading	0	0	0.000	
Material Loss	0.02	9	0.018	
Efflorescence	1.314	172	1.174	

Table 4. Overview of Damage Extent on the West Facade

Figure 5. Damage Atlas of the South Facade

Figure 6. Damage Atlas of the North Facade

Figure 7. Damage Atlas of the East Facade

Figure 8. Damage Atlas of the West Facade

4.2 Calculation of Damage Factors

The damage maps were drawn using the MMD method based on the defined grid system, as shown in Figures 9–12.As soiling, fading, and vegetation intrusion have relatively minor effects on the material pathological conditions of built heritage and are relatively easy to repair, soiling and fading were excluded from the classification in this phase of measurement.Therefore, six types of damage were measured using the MMD method: cracks, weathering, powdering, spalling, damage, and efflorescence. It is evident that when using a grid, the measured values of small-scale damage types—such as cracks—increase significantly.However, the 0.05 m × 0.05 m grid provides a closer approximation of the actual damage and enables more accurate quantification of anomalies.

South Facade	Facade Area (m^2)		187.31	
Pathological Manifestation	Indicated Area in Damage Map (m^2)	Indicated Area inMMD Damage Map (m^2)	FD (%)	FDt (%)
Crack	0.161	0.615	0.328	
Efflorescence	1.735	4.708	2.514	
Weathering	0.000	13.988	7.468	10.6
Spalling	0.319	0.380	0.203	73
Powdering	0.000	0.278	0.148	
Damage	0.563	0.023	0.012	

Table 5. Damage Scope of the South Facade Based on MMD Damage Map

North Facade	Facade Area (m^2)		177.33	
Pathological Manifestation	Indicated Area in Damage Map (m^2)	Indicated Area inMMD Damage Map (m^2)	FD (%)	FDt (%)
Crack	0.161	0.403	0.227	
Efflorescence	1.735	1.542	0.870	
Weathering	0.000	10.450	5.893	8.29
Spalling	0.319	0.868	0.490	9
Powdering	0.000	1.350	0.761	
Damage	0.563	0.103	0.058	

Table 6. Damage Scope of the North Facade Based on MMD Damage Map

East Facade	Facade Area (m^2)		111.72	
Pathological Manifestation	Indicated Area in Damage Map (m^2)	Indicated Area inMMD Damage Map (m^2)	FD (%)	FDt (%)
Crack	0.161	0.248	0.222	
Efflorescence	1.735	0.840	0.752	
Weathering	0.000	7.785	6.968	8.95
Spalling	0.319	0.110	0.099	2
Powdering	0.000	0.488	0.437	
Damage	0.563	0.530	0.474	

Table 7. Damage Scope of the East Facade Based on MMD Damage Map

West Facade	Facade Area (m^2)		111.92	
Pathological Manifestation	Indicated Area in Damage Map (m^2)	Indicated Area in MMD Damage Map (m^2)	FD (%)	FDt (%)
Crack	0.161	0.178	0.159	
Efflorescence	1.735	2.124	1.898	
Weathering	0.000	2.165	1.934	4.55
Spalling	0.319	0.255	0.228	1
Powdering	0.000	0.333	0.298	
Damage	0.563	0.038	0.034	

Table 8. Damage Scope of the West Facade Based on MMD Damage Map

Tables 5-8 present two sets of data: one derived from the actual damage maps and the other from the MMD-based damage maps, describing the occurrence of different types of damage and the corresponding FD and FDt values for each facade. The indicated damage areas in the actual damage map and the MMD-based damage map are distinct, as the former records the actual occurrence of damage, while the latter is based on grid-unit calculations where damage is present.For the calculation, the selection principles are defined as follows: for linear damage types such as cracks, if the length of damage

within a grid cell is greater than or equal to one side of the grid, the full cell area is counted; otherwise, it is excluded. For areal damage types such as spalling and weathering, if the damaged area within a grid cell is greater than or equal to half of the cell’s area, the full area is included; if less than half, it is excluded.

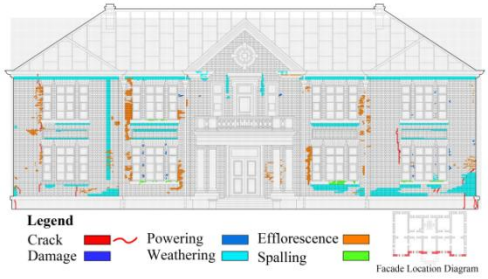

Figure 9. MMD Damage Map of the South Facade

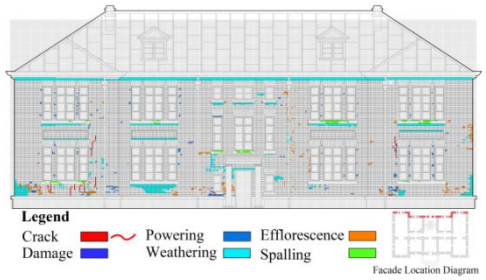

Figure 10. MMD Damage Map of the North Facade

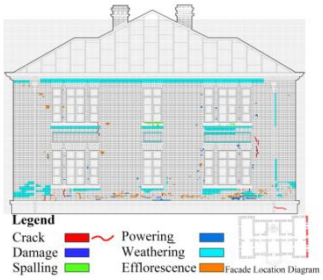

Figure 11. MMD Damage Map of the East Facade

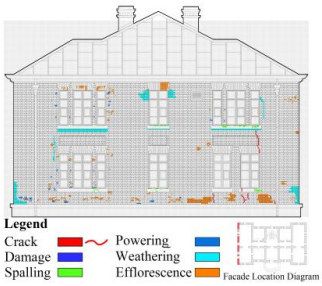

Figure 12. MMD Damage Map of the West Facade

In the comparative analysis between actual damage maps and MMD damage maps regarding pathological manifestations, contamination and discoloration are excluded from the MMD classification, making weathering and efflorescence the most frequently occurring types of damage. Damage that occurs at a small scale but is distributed across the entire facade—such as spalling, powdering, and cracking—shows increased severity. This is related to the overlapping of damaged grids, as the extent to which a given pathological manifestation affects its respective area must be considered.

From the facade damage of historic buildings, it is not difficult to observe that the Damage Factor only reflects the overall severity of damage on the facade but does not indicate the degree of damage concentration. This necessitates the analysis of the FDr, which takes into account the influencing factors of each affected region and considers all types of damage present within that space.

Figure 13 Regional Damage Mapping of the South Facade

Figure 14 Regional Damage Mapping of the North Facade

Figure 15 Regional Damage Mapping of the East Facade

Figure 16 Regional Damage Mapping of the West Facade

As shown in Figures 13–16 and Table 9, it is evident that the results of the FDr are directly influenced by the size of the region.The findings at this stage indicate that the region with the most frequent damage occurrence is the Continuous Wall: 6.289% on the south facade, 4.489% on the north facade, 6.245% on the east facade, and 2.899% on the west facade.The results demonstrate that FDr is directly affected by the size of the region; if the area is too large or too small, it can distort the actual severity of the damage in that region, with larger areas showing a higher degradation rate compared to smaller ones.To

correct the disproportionality within each region, it is necessary to apply adjustments and scaling by calculating the CCr. The FDrc, derived from adjusting FDr using CCr, provides a more objective and accurate representation of the actual damage severity in facade regions, independent of specific damage types.

	Total Area of South Facade (m^2)	187.31	Total Area of North Facade (m^2)	177.33
Region	Damage Coverage Area in Region (m^2)	FDr (%)	Damage Coverage Area in Region (m^2)	FDr (%)
Continuous Wall	11.780	6.289	7.961	4.489
Opening Interstory	2.560	1.367	2.285	1.289
Transition Zone	1.190	0.635	0.605	0.341
Corners and Edges	4.643	2.479	5.539	3.127
Cantilevered Element	0.000	0.000	0.000	0.000
	Total Area of East Facade (m^2)	111.72	Total Area of West Facade (m^2)	111.92
Region	Damage Coverage Area in Region (m^2)	FDr (%)	Damage Coverage Area in Region (m^2)	FDr (%)
Continuous Wall	6.977	6.245	3.245	2.899
Opening Interstory	0.338	0.303	1.065	0.952
Transition Zone	0.307	0.275	0.103	0.092
Corners and Edges	1.732	1.550	0.695	0.621
Cantilevered Element	0.000	0.000	0.000	0.000

Table 9 FDr Based on MMD

SouthFacade	Facade Area (m^2)		187.31	
Region Name	Region Area (m^2)	CCr	Damage Coverage Area (m^2)	FDrc (%)
Continuous Wall	79.200	0.119	11.780	0.748
Opening Interstory	28.889	0.325	2.560	0.444
Transition Zone	9.400	1.000	1.190	0.635
Corners and Edges	50.597	0.186	4.643	0.461
Cantilevered Element	19.224	/	/	/

Table 10. CCr and FDrc for the South Facade

North Facade	Facade Area (m^2)		177.33	
Region Name	Region Area (m^2)	CCr	Damage Coverage Area (m^2)	FDrc (%)
Continuous Wall	91.954	0.119	7.961	0.534
Opening Interstory	29.253	0.376	2.285	0.485
Transition Zone	10.900	1.000	0.605	0.341
Corners and Edges	42.209	0.258	5.539	0.807
Cantilevered Element	3.014	/	/	/

Table 11 CCr and FDrc of the North Facade

East Facade	Facade Area (m^2)		111.72	
Region Name	Region Area (m^2)	CCr	Damage Coverage Area (m^2)	FDrc (%)
Continuous Wall	62.052	0.124	6.977	0.774
Opening Interstory	14.960	0.513	0.338	0.155
Transition Zone	7.675	1.000	0.307	0.275
Corners and Edges	27.033	0.284	1.732	0.440
Cantilevered Element	/	/	/	/

Table 12 CCr and FDrc of the East Facades

West Facade	Facade Area (m^2)		111.92	
Region Name	Region Area (m^2)	CCr	Damage Coverage Area (m^2)	FDrc (%)
Continuous Wall	61.890	0.124	3.245	0.359
Opening Interstory	15.320	0.501	1.065	0.477
Transition Zone	7.675	1.000	0.103	0.092
Corners and Edges	27.035	0.284	0.695	0.176
Cantilevered Element	/	/	/	/

Table 13 CCr and FDrc of the West Facade

AllFacades	Facade Area (m^2)		588.28	
Region Name	Region Area (m^2)	CCr	Damage Coverage Area (m^2)	FDrc (%)
Continuous Wall	295.096	0.075	29.963	0.382
Opening Interstory	88.422	0.252	6.248	0.268
Transition Zone	35.650	0.624	2.205	0.234
Corners and Edges	146.874	0.152	12.609	0.326
Cantilevered Element	22.238	1.000	0.000	0.000

Tables 14 CCr and FDrc for All Facades

The table presents the final values of the CCr and the FDrc.The FDrc represents the relative and objective degree of degradation (damage) in each region and allows for an objective evaluation of the material damage severity in historic buildings.The magnitude of the value indicates the extent of material damage on the facade, reflecting the severity of degradation caused by cumulative damage in different regions.

As shown in Tables 10 to 13, the most severely damaged area on the south facade is the Continuous Wall, with an FDrc of 0.748%, while the Continuous Wall on the east facade is even more severely damaged, with an FDrc of 0.774%, requiring urgent intervention to prevent further deterioration.On the west facade, the most severely damaged area is around the Openings, with an FDrc of 0.477%, which warrants heightened attention.

Figure 17 illustrates the comparative analysis of overall It can be observed that the extent of damage varies among different regions of each facade.damage severity across all facades.For

example, the Continuous Wall on the east facade suffers the most severe damage; the areas around the Openings and the Interstory Transition Zone on the north facade, as well as the Corners and Edges on the east facade, also exhibit significant degradation. These areas should be prioritized for further intervention and preventive measures to avoid continued deterioration.Except for the Opening area, the other regions on the west facade show relatively low damage severity and require only enhanced routine maintenance.

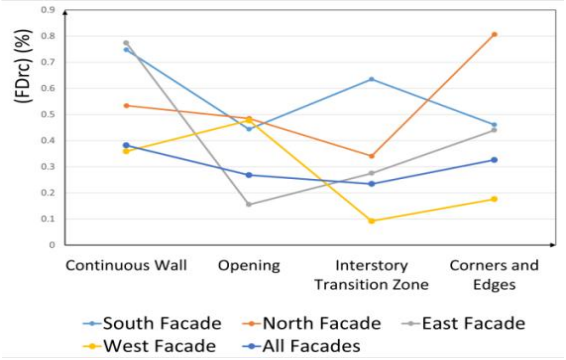

Figure 17. FDrc across Facades

5. Outlook

In the past, the registration and updating of basic information on architectural heritage have paid insufficient attention to the precise acquisition of damage data; however, digital damage measurement technologies, characterized by their accuracy, efficiency, and speed, facilitate the timely updating of damage information, enable dynamic monitoring of the health condition of architectural heritage, and support the establishment of a comprehensive digital pathological archive.

This study introduces the MMD to statistically and quantitatively analyze the damage conditions of facade materials in masonry architectural heritage, and visualizes damage conditions in real time through the form of damage mapping.By collecting damage data in real time, the MMD method analyzes the distribution patterns of facade deterioration in architectural heritage and objectively evaluates the health condition of masonry facade materials through the calculation of damage factors.Its advantage lies in utilizing simple and non-destructive measurement techniques to compute and capture the distribution characteristics of material damage on building facades.The study will employ the MMD to conduct multiple measurements and updates of facade material damage data across different years, analyze the developmental characteristics of various damage types, describe the deterioration patterns in detail based on calculated damage factors, and make scientifically sound predictions regarding the progression of different pathologies.

Reference

Jansen, M.; Toubekis, G.; Walther, A.; Döring- Williams, M.; Mayer, I., 2008. Laser scan measurement of the niche and virtual 3D representation of the Small Buddha in Bamiyan. In: Posluschny, A.; Lambers, K.; Herzog, I. (eds.), Proc. 35th Int. Conf. on Computer Applications and Quantitative Methods in Archaeology(CAA),pp.83-90.doi:10.11588/propylaeumdok.00000531

Wang, M., 2011. Application of 3D laser scanning technology in surveying ancient architecture of the Forbidden City. Palace Mus. J., (6), 143–156.

Edis, E.; Flores- Colen, I.; de Brito, J., 2014. Passive thermographic detection of moisture problems in façades with adhered ceramic cladding. Constr. Build. Mater., 51, 187–197. doi:10.1016/j.conbuildmat.2013.10.085

Theodorakeas, P.; Avdelidis, N.P.; Cheilakou, E.; Koui, M., 2014. Quantitative analysis of plastered mosaics by means of active infrared thermography. Constr. Build. Mater., 73, 417–425. doi:10.1016/j.conbuildmat.2014.09.050

Silveira da Costa, V.; Montagna da Silveira, A.; da Silva Torres, A., 2021. Evaluation of degradation state of historic building facades through qualitative and quantitative indicators: Case study in Pelotas, Brazil. Int. J. Archit. Herit., 16(11), 1642–1665. doi:10.1080/15583058.2021.1901161

Gaspar, P.L.; de Brito, J., 2005. Mapping defect sensitivity in external mortar renders. Constr. Build. Mater., 19(8), 571–578. doi:10.1016/j.conbuildmat.2005.01.014

Franković, M.; Novaković, N.; Matović, V., 2015. Damage quantification of built stone on Dark Gate (Belgrade, Serbia): sample of damage index application for decay rate evaluation. Environ. Earth Sci., 73(10), 6181–6193. doi:10.1007/s12665-015-3843-z

Janvier- Badosa, S.; Beck, K.; Brunetaud, X.; Al- Mukhtar, M., 2013. Historical study of Chambord Castle: basis for establishing the monument health record. Int. J. Archit. Herit., 7(3), 247–260. doi:10.1080/15583058.2011.634959

Carvalho, G.B., 2018. Proposal for graphical representation of damage maps on exposed reinforced concrete facades in modernist architecture. Master’s thesis, Universidade de Brasília, Brasília, Brazil.

Silva, M.N.B., 2014. Quantitative evaluation of degradation and service life of facade coatings: application to Brasília/DF’s case. Ph.D. thesis, Universidade de Brasília, Brasília, Brazil.

De Souza, J.S.; Bauer, E.; Nascimento, M.L.M.; Capuzzo, V.M.S.; Zanoni, V.A.G., 2016. Study of damage distribution and intensity in regions of the facade. J. Build. Pathol. Rehabil., 1(1), 3. doi:10.1007/s41024-016-0003-8

Bauer, E.; Piazzarollo, C.B.; de Souza, J.S.; dos Santos, D.G., 2020. Relative importance of pathologies in the severity of façade degradation. J. Build. Pathol. Rehabil., 5(1), 7. doi:10.1007/s41024-020-0072-6

Bauer, E.; de Souza, J.S.; Piazzarollo, C.B., 2020. Application of the degradation measurement method in the study of façade service life. In: Delgado, J.M.P.Q. (Ed.), Building Pathology, Durability and Service Life, Building Pathology and Rehabilitation, Vol. 12. Springer, Cham, pp. 105–119. doi:10.1007/978-3-030-47302-0_5

Sousa, V.; Almeida, N.; Meireles, I.; de Brito, J., 2011. Anomalies in wall renders: overview of the main causes of degradation. Int. J. Archit. Herit., 5(2), 198–218. doi:10.1080/15583050903487633